

November 02, 2009

## Time domain analyses of the converse magnetoelectric effect in a multiferroic metallic glass-relaxor ferroelectric heterostructure

Yajie Chen  
*Northeastern University*

Anton L. Geiler  
*Northeastern University*

Trifon Fitchorov  
*Northeastern University*

Carmine Vittoria  
*Northeastern University*

V. G. Harris  
*Northeastern University*

---

### Recommended Citation

Chen, Yajie; Geiler, Anton L.; Fitchorov, Trifon; Vittoria, Carmine; and Harris, V. G., "Time domain analyses of the converse magnetoelectric effect in a multiferroic metallic glass-relaxor ferroelectric heterostructure" (2009). *Electrical and Computer Engineering Faculty Publications*. Paper 134. <http://hdl.handle.net/2047/d20002305>

## Time domain analyses of the converse magnetoelectric effect in a multiferroic metallic glass-relaxor ferroelectric heterostructure

Yajie Chen, Anton L. Geiler, Trifon Fitchorov, Carmine Vittoria, and V. G. Harris

Citation: *Appl. Phys. Lett.* **95**, 182501 (2009); doi: 10.1063/1.3258023

View online: <http://dx.doi.org/10.1063/1.3258023>

View Table of Contents: <http://apl.aip.org/resource/1/APPLAB/v95/i18>

Published by the [American Institute of Physics](http://www.aip.org).

---

### Related Articles

Comparative study on aging effect in BiFeO<sub>3</sub> thin films substituted at A- and B-sites  
*Appl. Phys. Lett.* **99**, 262901 (2011)

Fabrication, electrical characterization, and modeling of fully-porous pn junctions  
*J. Appl. Phys.* **110**, 036106 (2011)

Communication: Effective temperature and glassy dynamics of active matter  
*J. Chem. Phys.* **135**, 051101 (2011)

Role of surface vibration modes in Si nanocrystals within light emitting porous Si at the strong confinement regime  
*J. Appl. Phys.* **110**, 023527 (2011)

Decomposition pathways in age hardening of Ti-Al-N films  
*J. Appl. Phys.* **110**, 023515 (2011)

---

### Additional information on *Appl. Phys. Lett.*

Journal Homepage: <http://apl.aip.org/>

Journal Information: [http://apl.aip.org/about/about\\_the\\_journal](http://apl.aip.org/about/about_the_journal)

Top downloads: [http://apl.aip.org/features/most\\_downloaded](http://apl.aip.org/features/most_downloaded)

Information for Authors: <http://apl.aip.org/authors>

## ADVERTISEMENT



## Time domain analyses of the converse magnetoelectric effect in a multiferroic metallic glass-relaxor ferroelectric heterostructure

Yajie Chen,<sup>a)</sup> Anton L. Geiler, Trifon Fitchorov, Carmine Vittoria, and V. G. Harris  
*Department of Electrical and Computer Engineering and Center for Microwave Magnetic Materials and Integrated Circuits, Northeastern University, Boston, Massachusetts 02115-5000, USA*

(Received 8 September 2009; accepted 12 October 2009; published online 3 November 2009)

The dynamic time domain response of the converse magnetoelectric effect in a multiferroic Metglas<sup>®</sup>/Pb(Mg<sub>1/3</sub>Nb<sub>2/3</sub>)O<sub>3</sub>-PbTiO<sub>3</sub> (PMN-PT) heterostructure, under the application of a square waveform electric field excitation of 8 kV/cm at a frequency of 0.4 Hz, is reported. The relaxation behavior followed a stretched power-law function allowing the calculation of an intrinsic time constant. Aging behavior of magnetoelectric coupling was observed after polarization switching of 1000 cycles. These phenomena are predominantly attributed to the temporal response of polarization within the PMN-PT crystal. Results elucidate the dynamic properties of relaxor-based multiferroic heterostructures and importantly define operational constraints for low frequency device operation. © 2009 American Institute of Physics. [doi:10.1063/1.3258023]

Developments in modern electronics technologies have focused on performance figures of merit, miniaturization, and more recently, enhanced multifunctional properties. Spurred in part by the latter, the field of multiferroic (MF) materials and heterostructures, which demonstrate the magnetoelectric (ME) effect, has experienced great interest, activity, and progress in both fundamental physics as well as development toward practical engineering applications.<sup>1</sup> In general, MF materials are categorized as either single phase or multiphase/multicomponent structures. As a result, most activity has focused on MF heterostructures that exhibit large room temperature ME effects and are relatively simple in construction and cost-effective in fabrication. Owing to a wide variety of potential applications, MF heterostructures provide an opportunity to realize rapid insertion to practical multifunctional electronic systems.<sup>2-4</sup>

Conventionally, the ME effect is described as an electric polarization response to an applied magnetic field, or conversely, a magnetic spin polarization response to an applied electric field. The latter is referred to as the *converse* ME (CME) effect and is a focus of the present study. It is noteworthy that either of these effects may be of great practical value in such applications as: ac and dc magnetic field sensors, current sensors, transformers and gyrators, microwave resonant devices including ferromagnetic resonators and filters, magnetic field generators, hybrid spintronic-MF devices such as MRAM memory elements, and electric field tunable microwave and millimeter-wave devices (e.g., phase shifters, filters, antennas, etc.).<sup>5,6</sup>

When considering the transference of prototype to practical device, one must examine and understand the dynamic response of the MF heterostructure, in particular the stability of the CME (or ME) effect in frequency and time domains. A variety of ME devices operate over a broad range of frequencies.<sup>7</sup> Although the importance of dynamic response cannot be underestimated, presently there is a lack of knowledge base for such behavior in most MF heterostructures.<sup>8-10</sup> Although preliminary research<sup>7,11,12</sup> has been conducted on the low frequency ME response in lead zirconate titanate

(PZT) and lead magnesium niobate-lead titanate (PMN-PT)-based structures, it remains unclear how the CME effect will respond dynamically to applied electric fields.

In this letter, we report on the analyses of time domain and aging effects of the CME coupling based on a laminated heterostructure consisting of a ferromagnetic magnetostrictive Metglas<sup>®</sup> ribbon affixed to a PMN-PT substrate. The amorphous Metglas<sup>®</sup> ribbon, i.e., Metglas Inc. 2605C0, has a thickness of 23–30 μm, saturation magnetization  $4\pi M_s = 18$  kG, coercivity  $H_c = 0.15$  Oe, and saturation magnetostriction coefficient  $\lambda_s = 35$  ppm. The  $(1-x)\text{Pb}(\text{Mg}_{1/3}\text{Nb}_{2/3})\text{O}_3-x\text{PbTiO}_3$  single crystal, features anisotropic in-plane piezoelectric coefficients [i.e., in the (011) plane],  $d_{31} = -1800$  pC/N and  $d_{32} = 900$  pC/N, while poled along with (011). Here, we employ a (011)-type PMN-PT crystal of dimensions  $L \times W \times T = 5 \times 5 \times 0.5$  mm. This MF heterostructure was designed to operate in the L-T ME coupling mode, i.e., longitudinal magnetized and transverse polarized. The two components were laminated using quick curing ethyl cyanoacrylate. Measurement of the CME coupling was performed in the geometry and field configuration depicted in inset (a) of Fig. 1. An external magnetic field (H) was applied along the (011) ( $d_{32}$ ) direction of the PMN-PT crystal, where the (011) ( $d_{33}$ ) aligns perpendicular to the heterostructure plane. An optimal thickness ratio of magnetic to ferroelectric components is a prerequisite to obtaining large CME. For the MF heterostructure of the present study, the ideal thickness ratio was 0.05, or 25 μm Metglas<sup>®</sup> ribbon to 500 μm PMN-PT crystal.

The magnetic properties of the heterostructure were measured using a vibrating sample magnetometer (VSM). The low frequency ME response was measured by VSM, while the PMN-PT slab was electrically driven by a square waveform generated by a function generator and high voltage power amplifier.

Figure 1 presents static magnetic properties measured as hysteresis loops with (dash line) and without (solid line) the application of electric field. The magnetic ribbon bonded to the PMN-PT substrate exhibits a saturation magnetization as  $4\pi M_s$  of 17.8 kG, and coercivity ( $H_c$ ) of 2.1 Oe in the ab-

<sup>a)</sup>Electronic mail: y.chen@neu.edu.

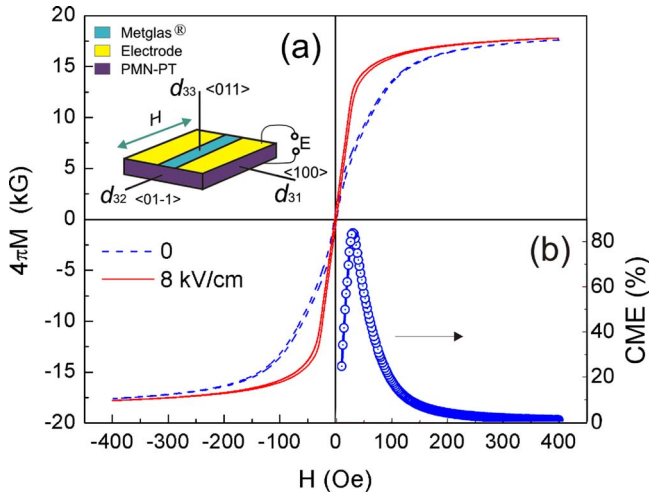


FIG. 1. (Color online) Magnetic hysteresis loops for a Metglas<sup>®</sup>/PMN-PT heterostructure with (solid curve) and without (dash curve) the application of electric field. Inset (a) is a schematic diagram of the MF heterostructure depicting measurement geometries, and (b) the dependence of CME effect in response to applied magnetic fields.

sence of an electric bias field. The coercivity deduced from the data of Fig. 1 is an apparent value which is strongly dependent upon the stress state of the structure imposed by the bonding of the ribbon to the PMN-PT substrate. This is not the intrinsic value for the Metglas<sup>®</sup> material. The application of the drive field, 8 kV/cm, causes significant changes in the magnetic hysteresis loop, and in fact, induces the material to become substantially softer (in the magnetic sense) with coercivity reduced by 26% (i.e., 1.56 Oe) and permeability increased nearly 200% relative to the unbiased state. Because both stress ( $\sigma$ ) and magnetostriction coefficient ( $\lambda$ ) are positive, magnetoelastic theory [Eq. (1)],

$$F_{\sigma} = -\frac{3}{2}\lambda \cdot \sigma \cdot \cos \theta, \quad (1)$$

where  $F_{\sigma}$  represents the magnetoelastic energy and  $\theta$  denotes the angle between stress and magnetization, predicts the stress-induced field will align parallel the applied magnetic field. Results of Fig. 1 are fully consistent with this calculation. Magnetic field dependence of the CME effect is illustrated as the inset (b) to Fig. 1. CME is defined here as  $\text{CME} = [M(E) - M(0)]/M(0)$ , where  $M(E)$  and  $M(0)$  represent magnetizations with and without the application of electric field ( $E$ ), respectively. The inset to Fig. 1 indicates that the maximum CME effect occurs at  $H \sim 30$  Oe, presumably corresponding to the maximum value in the magnetostriction derivative,  $(\partial\lambda/\partial M)_{\text{max}}$ .<sup>13</sup>

Figure 2 displays the CME magnitude in different time domains for the heterostructure under the excitation of a square waveform electric field of 8 kV/cm at a frequency of 0.4 Hz. Due to the application of a dc offset, the square wave field switches from 0 to 8 kV/cm without change in polarity. Figure 2(a) illustrates the CME magnitude versus time for the initial 100 cycles applied to a prepoled PMN-PT substrate. It is particularly noteworthy that the CME value increases with increasing number of cycles. Within the time domain of 100 s, there is an increase in  $\sim 4\%$  in the CME effect, i.e., from 65.6% to 68.8%. With increasing time domain, the CME effect reveals a clear time dependence. Figures 2(b)–2(d) present CME versus time for different time domains, i.e., after 100, 500, and 2500 s, respectively. Ap-

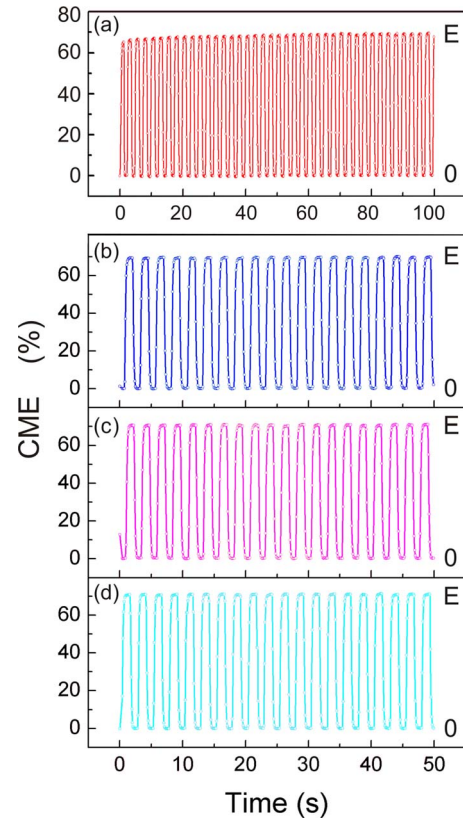


FIG. 2. (Color online) Variation in CME effect with time in different time domains for the Metglas<sup>®</sup>/PMN-PT heterostructure. A square waveform electric field ( $E$ ) of 8 kV/cm was applied. (a) Initial 100 s, (b) 50 s after 100 s, (c) 50 s after 500 s, and (d) 50 s after 2500 s.

plying the same observation time window of 50 s relative to the three time domains, we measure an enhancement in the CME effect 69.6%, 69.9%, and 70.1% corresponding to the time after 100, 500, and 2500 s, respectively. However, the CME effect is nearly independent of time within each observation window of 50 s; A quantitative calculation indicates changes in 0.1%–0.3% in the CME effect. Such variations are negligible compared to the enhancement in the CME effect for the initial observation window of 100 s [Fig. 2(a)].

Figures 3(a) and 3(b) display variations in CME values with cycles and time relative to the initial application of the square waveform  $E$ -field. Figure 3(a) indicates an enhancement in CME with number of cycles. It reflects two physical phenomena, that is, the polarization relaxation and memory effect in the heterostructure. By means of random-field theory, it is well-known that for many disordered ferroelectrics the correlation of polarization with time follows a stretched power-law function as presented below:<sup>14</sup>

$$P(t) = A \exp \left\{ \left[ -a \ln \left( \frac{t}{\tau} \right) \right]^n \right\}, \quad (2)$$

where  $\tau$  and  $n$  denote the time constant and dimensionality, respectively. In the present experiment, we fit the measured CME values to Eq. (2). The fitting results yield a  $\tau$  of 0.12 s, derived from the fit to the data of Fig. 3(b). The ability to fit CME to the same formalism employed to describe relaxation in relaxor ferroelectrics supports our contention that  $\tau$  is primarily determined by the relaxation in the PMN-PT crystal. An important fact is that the time constant of polarization

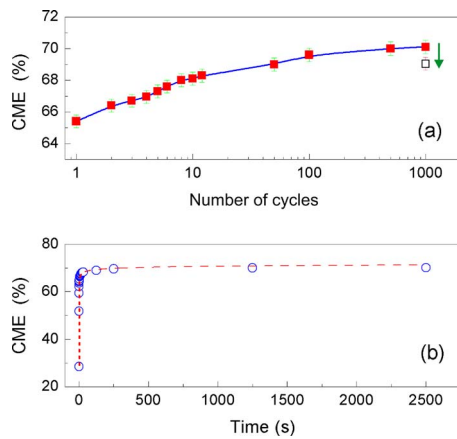


FIG. 3. (Color online) Variation in CME with (a) number of E-field cycles, and (b) time after initial excitation of the Metglas<sup>®</sup>/PMN-PT heterostructure. In panel (a) the square hollow symbol represents the measured value after termination of continuous cycling at 1000 cycles followed by a rest period of 60 min. In panel (a) the solid curve is a guide to the eyes, whereas in (b) the dash curve is the best fit to Eq. (2).

switching strongly depends upon the electric field strength, whereas the coercive field ( $E_c$ ) becomes a critical field that affects relaxation time.<sup>15</sup>

Another observation of potential importance is that CME coupling is nearly independent of measurement time while the heterostructure experienced more than 1000 E-field cycles. A CME value of  $\sim 69\%$ , somewhat lower than that measured for the same sample during the first series of cycles, remains constant, as depicted in Fig. 3(a). These results imply dynamic switching of applied electric field introduces an *aging* effect for this heterostructure, in addition to the measured polarization relaxation. The effect of aging on the sample cycled for 1000 times is denoted by the arrow presented in Fig. 3(a). In principle, these phenomena may be attributed to the entire heterostructure, including: magnetic relaxation of the Metglas<sup>®</sup> ribbon, electronic/ionic relaxation of the PMN-PT crystal, and mechanical relaxation of the bonding interface. However, we propose that the ferroelectric relaxor is primarily responsible for the time domain response and aging effect of the CME, which is supported in part by previous work on the relaxation behavior of PMN-PT crystals.<sup>16,17</sup> Aging behavior has been attributed to ferroelec-

triclike polar nanoregions (PNRs).<sup>18</sup> Very recently, experiments indicate that the distinctive aging behavior of glassy kinetics are due to degrees of freedom other than those associated with PNR polarization orientation.<sup>19</sup> In the present case, since an electric field of 8 kV/cm is insufficient to fully saturate the ferroelectric crystal, we conjecture that spinglasslike aging dominates this heterostructure. These findings present challenges to realizing practical low frequency multifunctional devices based on MF heterostructures. In particular, the heterostructure studied here does not experience saturation of the CME effect until nearly 1000 E-field cycles which may provide limitations in their use in instantaneous mode applications.

<sup>1</sup>J. Scott, *Nature Mater.* **6**, 256 (2007).

<sup>2</sup>Y. Chen, J. Gao, T. Fitchorov, Z. Cai, K. S. Ziemer, C. Vittoria, and V. G. Harris, *Appl. Phys. Lett.* **94**, 082504 (2009).

<sup>3</sup>C. W. Nan, M. I. Bichurin, S. Dong, and D. Viehland, *J. Appl. Phys.* **103**, 031101 (2008).

<sup>4</sup>G. Srinivasan, E. T. Rasmussen, and R. Hayes, *Phys. Rev. B* **67**, 014418 (2003).

<sup>5</sup>M. Vopsaroiu, J. Blackburn, and M. G. Cain, *Mater. Res. Soc. Symp. Proc.* **1161**, 574174 (2009).

<sup>6</sup>Y. Chen, J. Gao, J. Lou, S. D. Yoon, A. L. Geiler, M. Nedoroscik, D. Heiman, N. X. Sun, C. Vittoria, and V. G. Harris, *J. Appl. Phys.* **105**, 07A510 (2009).

<sup>7</sup>X. Dong, J. Y. Zhai, Z. P. Xing, J. F. Li, and D. Viehland, *Appl. Phys. Lett.* **86**, 102901 (2005).

<sup>8</sup>M. Liu, O. Obi, J. Lou, Y. Chen, Z. Cai, S. Stoute, M. Espanol, M. Lew, X. Situ, K. S. Ziemer, V. G. Harris, and N. X. Sun, *Adv. Funct. Mater.* **19**, 1 (2009).

<sup>9</sup>Y. Chen, J. Wang, M. Liu, J. Lou, N. X. Sun, C. Vittoria, and V. G. Harris, *Appl. Phys. Lett.* **93**, 112502 (2008).

<sup>10</sup>Y.-Y. Song, J. Das, P. Krivosik, N. Mo, and C. E. Patton, *Appl. Phys. Lett.* **94**, 182505 (2009).

<sup>11</sup>Y. J. Wang, S. W. Or, H. L. W. Chan, X. Y. Zhao, and H. S. Luo, *Appl. Phys. Lett.* **92**, 123510 (2008).

<sup>12</sup>K. E. Kamentsev, Y. K. Fetisov, and G. Srinivasan, *Tech. Phys.* **52**, 727 (2007).

<sup>13</sup>M. J. Sablik, S. W. Rubin, L. A. Riley, D. C. Jiles, D. A. Kaminski, and S. B. Biner, *J. Appl. Phys.* **74**, 480 (1993).

<sup>14</sup>I. Imry and S. Ma, *Phys. Rev. Lett.* **35**, 1399 (1975).

<sup>15</sup>D. Viehland and J. F. Li, *Philos. Mag.* **84**, 1969 (2004).

<sup>16</sup>X. J. Lou, *J. Appl. Phys.* **105**, 024101 (2009).

<sup>17</sup>E. V. Colla, L. K. Chao, M. B. Weissman, and D. D. Viehland, *Phys. Rev. Lett.* **85**, 3033 (2000).

<sup>18</sup>A. A. Bokov and Z. G. Ye, *J. Mater. Sci.* **41**, 31 (2006).

<sup>19</sup>E. V. Colla, P. Griffin, M. Delgado, and M. B. Weissman, *Phys. Rev. B* **78**, 054103 (2008).